Spectrochimica Acta. Vol. 44A, No. 4, pp. 409–422. 1988.
Printed in Great Britain.

0584–8539/88 $3.00 + 0.00

The vibrational spectra, molecular structure and conformation of organic azides—IX. Azidoethane*

C. J. NIELSEN,† K. KOSA,‡, H. PRIEBE§ and C. E. SJØGREN‖
Department of Chemistry, University of Oslo, P.O. Box 1033, Blindern, 0315 Oslo 3, Norway

(*Received* 4 *September* 1987; *accepted* 24 *September* 1987)

Abstract—A safe method for the synthesis of azidoethane from ethylbromide is given and ^{1}H and ^{13}C NMR data are reported.

The i.r. and Raman spectra of azidoethane have been recorded in the region 4000–40 cm^{-1} and interpreted in terms of two conformers, *anti* and *gauche*, present in the vapour and in the liquid and of the *gauche* conformer in the crystalline solid. Matrix isolation studies reveal the *gauche* conformation to be the more stable in argon and in nitrogen matrices and probably also more stable in the vapour. The enthalpy difference between the conformers is calculated to be $\Delta H^0_{a\to g}$ (N_2 matrix) $\approx \Delta H^0_{a\to g}$ (vap.) $= -0.56(10)$ kJ mol^{-1}, and the barrier to rotational isomerism (*anti* → *gauche*) as 9.0(10) kJ mol^{-1} in the nitrogen matrix and less than 6 kJ mol^{-1} in the argon matrix. Careful Raman studies of the liquid at 140–290 K reveal the *gauche* conformation to be the more stable in the liquid phase as well, the enthalpy difference being $\Delta H^0_{a\to g}$ (liq.) $= -1.15$ (5) kJ mol^{-1}.

The majority of the fundamentals for both conformers have been assigned with the aid of normal coordinate calculations using previously developed scaled quantum mechanical force fields which are also presented.

INTRODUCTION

Azidoethane, synthesized for the first time in 1921 [1], is one of the more often studied organic azides. In our experience, the compound is relatively harmless although explosions have been reported during synthesis [2]. The dipole moment has been measured in benzene solution as 2.12 D [3, 4], the u.v. spectrum recorded [5, 6] and the ^{14}N NMR spectrum investigated [7–9]. CNDO/2 calculations have been performed on a series of organic azides, including azidoethane, in a study of the electronic structure of the azido group [10]. Of more interest in the present context, the Raman lines and a low-resolution i.r. spectrum have been published [11] and the vibrational fundamentals calculated [12]. More recently a study of the u.v. photolysis of matrix isolated azidoethane and azidoethane-d_5 was presented [13] but, unfortunately, the frequencies were not tabulated.

As part of our studies on organic azides [14–21] we have recently published the results of *ab initio* calculations on hydrazoic azid, azidomethane, azidoethane, azidoethene and azidomethanal [17]. Among the results were optimized geometries, complete harmonic force fields, i.r. intensities and scaled harmonic force fields, for which preliminary results from the present work were needed. However, only the azide part of the force fields was published [17] as it was felt desirable to present the complete force fields together with the spectral data.

With conformational possibilities around the C–N bond, azidoethane can exist in two conformations: *gauche* and *anti* (Fig. 1). According to the *ab initio* calculations [17] the *anti* conformation is the more stable, but the energy difference from the *gauche* conformation was calculated to be only 0.3 kJ mol^{-1}, i.e. much lower than the reliability of such calculations. Further, the barrier to rotational isomerism, which is also important to the present study, was calculated to be rather low, a mere 3.3 kJ mol^{-1}.

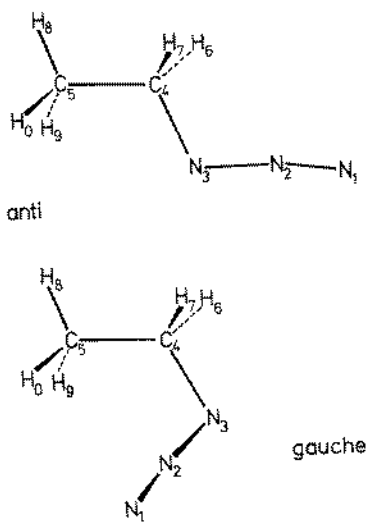

Fig. 1. Atomic numbering in the *anti* and *gauche* conformations of azidoethane. Note the transoid arrangement around N_2–N_3.

* Part VIII of this series is given as Ref. [21].

† Author to whom correspondence should be directed.

‡ On leave from Department of Physical Chemistry, Polytechnical University of Budapest, H-1521 Budapest, Hungary.

§ Present address: NYCOMED, P.O. Box 4220, Torshov, N-0401 Oslo 4, Norway.

‖ Present address: Center for Industrial Research, P.O. Box 124, Blindern, N-0314 Oslo 3, Norway.

As to the structure of the azide group in organic azides, most of the vapour phase studies [15, 16, 18–24] as well as theoretical studies [17, 25] conclude with a non-linear azide chain bent 5–10° from linearity in a transoid arrangement. The charge distribution in the azide chain is best described by the resonance structure (a) [17, 26]:

but in aliphatic azides neither of these would favour the *gauche* or the *anti* conformation.

EXPERIMENTAL

Preparative

Tetramethylguanidinium azide (12.65 g, 80 mmol) was dissolved in sulfolane (60 ml) and the solution degassed at 50° C for 2 h in vacuum. Ethylbromide (2.98 ml, 4.35 g, 40 mmol) dissolved in sulfolan (20 ml) was added to the solution at 50° C. After 2 h the product was sucked into a trap, cooled with liquid nitrogen, recondensed and dried by condensation through a U-shaped tube, which was partially filled with phosphorous pentoxide. Yield 2.4 g (84 %), m.p. *ca* 160 K. ^{1}H NMR [200 MHz, $CDCl_3$]: $\delta = 3.29$ (2H, *q*, $J = 7.27$, $-CH_2-$), 1.26 (3H, *t*, $-CH_3$). ^{13}C NMR [50.3 MHz, $CDCl_3$, 253 K]: $\delta = 46.07$ (C-1), 13.77 (C-2).

Spectra

Infra-red spectra of azidoethane were recorded on a Perkin–Elmer model 225 spectrometer (5000–200 cm^{-1}), with a Perkin–Elmer model 1750 interferometer (4000–400 cm^{-1}) and with a Bruker IFS 114C interferometer (4000–20 cm^{-1}). Vapour phase spectra were obtained using cells of 10 and 20 cm pathlengths equipped with windows of CsI and polyethylene, respectively. Spectra were also obtained of the neat liquid and of CCl_4 solutions at room temperature and of the solid at *ca* 80 K using cryostats cooled with liquid nitrogen. When the vapour was deposited onto a cold CsI or polyethylene window (*ca* 80 K), the solid always appeared crystalline. Further spectra of the molecule isolated in argon and nitrogen matrices at ratios varying from 1:500 to 1:1000 were recorded using a closed-cycle cryostat from Air Products.

The Raman spectra were recorded on a DILOR RTI 30 spectrometer (triple monochromator) interfaced to the Aspect 2000 data system of the Bruker FTIR. The 488-nm line of a CRL 52G and the 514.8-nm line of a Spectra Physics Model 2000 argon ion laser were used for excitation. Spectra were obtained of the liquid in a capillary tube of 2 mm i.d. The tube was inserted in a transparent Dewar [27] and cooled by a stream of nitrogen evaporating from a reservoir equipped with a heating element. Raman spectra of the cooled liquid, including semiquantitative polarization measurements, were obtained in the temperature range 140–290 K. At all temperatures down to 140 K, *ca* 20° supercooling, the liquid stayed non-viscous and appeared stable for hours in the laser beam. Below 140 K the sample always turned crystalline instantaneously. Spectra were also recorded of the solid formed by shock freezing the vapour on a copper block cooled by liquid nitrogen. As was the case in the analogous i.r. experiments, the solid formed upon deposition always seemed to be crystalline. As a safety precaution the laser power was kept below 150 m W at the sample.

RESULTS

Infra-red survey spectra of azidoethane as a vapour and liquid at room temperature are reproduced in Figs 2 and 3, while the Raman spectra of the cooled liquid and the crystalline solid are shown in Figs 4 and 5, respectively. A part of the Raman spectrum of the liquid at temperatures in the range 140–290 K is given in Fig. 6. The spectral data are collected in Table 1, which also includes our interpretation. The Raman spectrum of azidoethane published previously [11] has, apart from some of the strongest bands, virtually no resemblance to our spectrum and most probably the sample decomposed or polymerized during the photographic recording.

A few bands, present in the spectra of the vapour and the liquid, vanish in the spectra of the crystalline solid. They have been marked with asterisks in Table 1 and interpreted as evidence for the existence of two stable conformations of azidoethane. Further evidence for conformational equilibria is found in the i.r. spectra of matrix isolated azidoethane. A comparison between the nitrogen matrix spectra before and after annealing (Fig. 7) reveals that the bands corresponding to those missing in the spectra of the crystalline solid (and many others) decrease in intensity upon annealing, while the

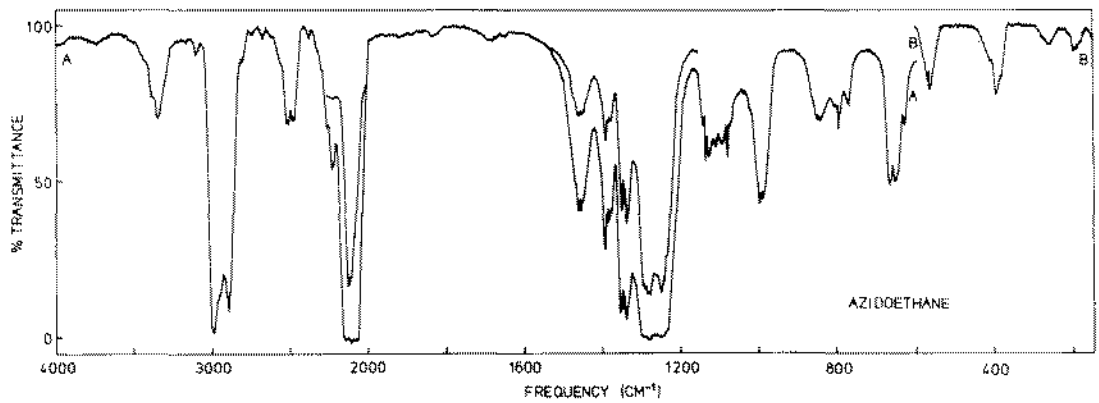

Fig. 2. Mid i.r. vapour spectrum of azidoethane. Pressure 50 Torr. (A) Pathlength 10 cm (CsI). (B) Pathlength 20 cm (polyethylene).

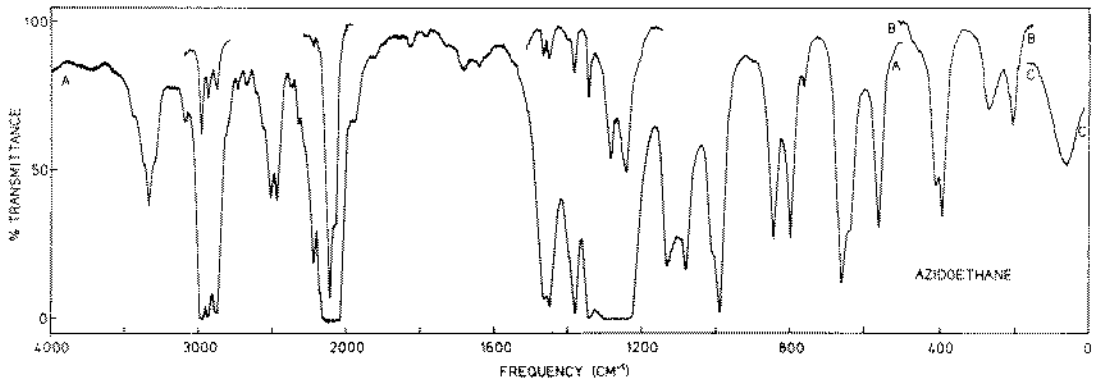

Fig. 3. Infra-red spectrum of azidoethane as a liquid at room temperature. (A) Pathlength 0.056 mm and thin film (KBr). (B) and (C) CCl_4 solution 3.5 and 12 μm beamsplitters, respectively.

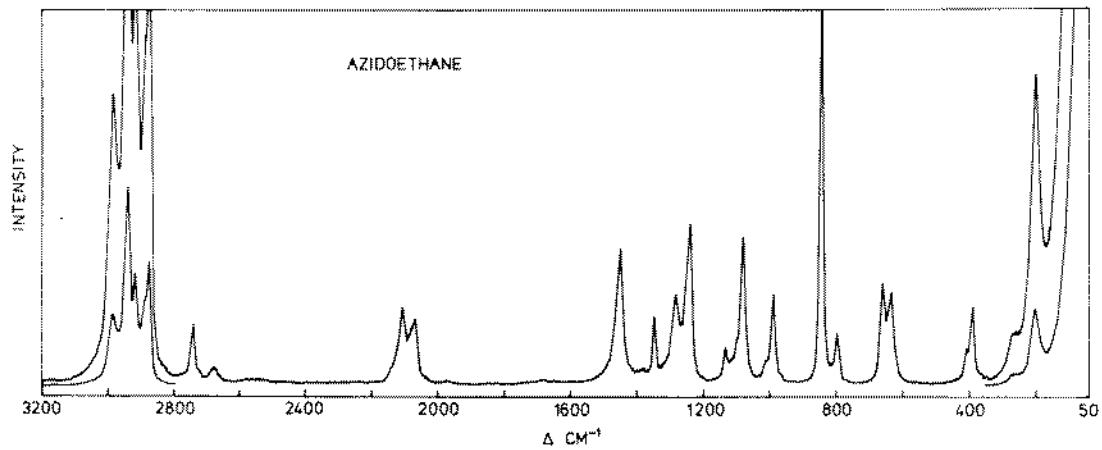

Fig. 4. Raman spectrum of azidoethane as a liquid at 260 K.

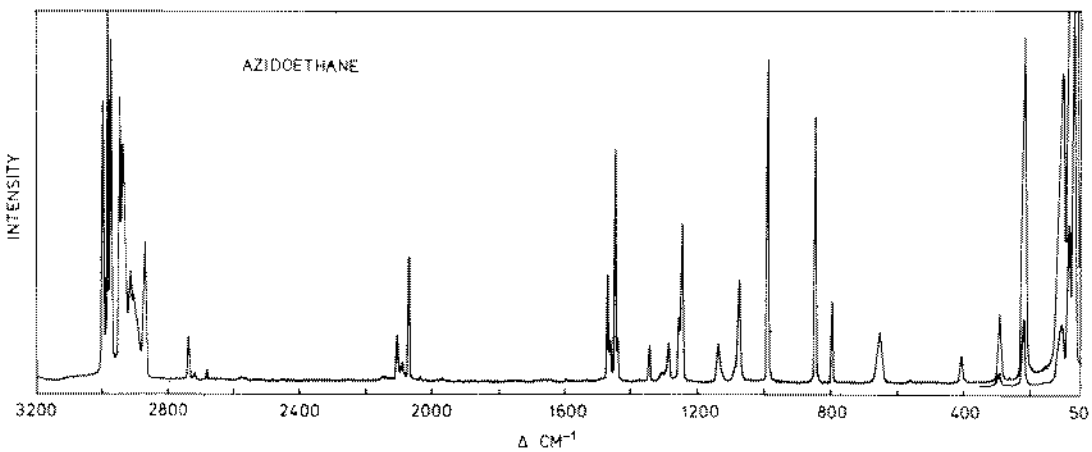

Fig. 5. Raman spectrum of azidoethane as a crystalline solid at *ca.* 80 K.

bands corresponding to those remaining in the crystal gain in intensity. The bands that show a clear variation in intensity upon annealing have been marked with arrows in Table 1. In contrast to this behaviour, the i.r. spectra of azidoethane isolated in argon matrices are quite different with respect to the band intensities. At the outset, they look almost like the annealed nitrogen spectra and they barely change upon annealing.

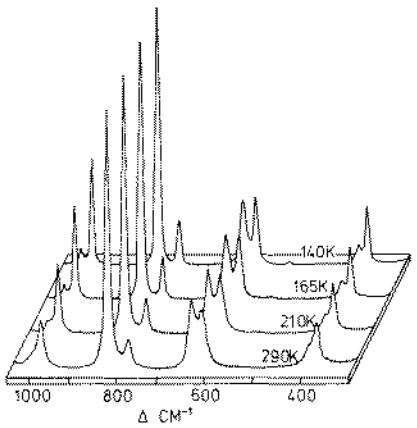

Fig. 6. Part of the Raman spectrum of azidoethane as a liquid in the temperature range 140–300 K.

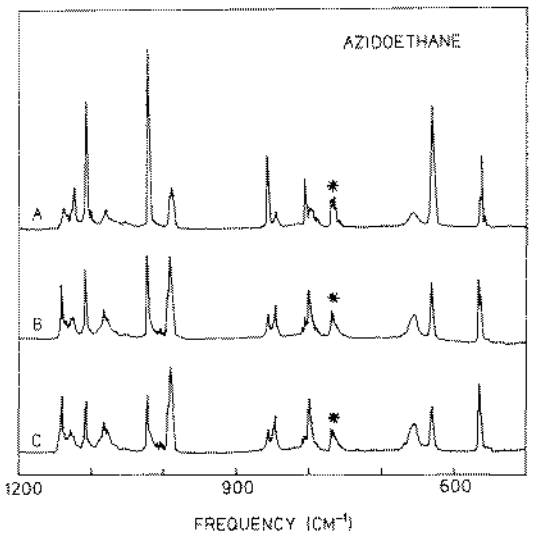

Fig. 7. Part of the i.r. spectra of azidoethane isolated in nitrogen matrices. Bands marked with asterisks (*) are due to an impurity of chloroform, $CHCl_3$.

DISCUSSION

Vibrational assignment

For the *anti* conformation of azidoethane with C_s symmetry the normal modes of vibration divide into $\Gamma_v = 15a' + 9a''$; the a' modes being polarized in the Raman effect and having i.r. vapour phase contours of the *A/B* hybrid type whereas the a'' modes should show typical *C*-type band contours. In the *gauche* conformation, C_1 symmetry, all bands should be polarized in the Raman effect and the i.r. vapour phase contours may be hybrids of *A*-, *B*-, and *C*-type. The theoretical vapour phase band contours for the *anti* and *gauche* conformers [28] are displayed in Fig. 8, the *PR*-separations being *ca*: 13, 13 and 22 cm^{-1} (*anti*) and 16, 12 and 20 cm^{-1} (*gauche*) for the *A*-, *B*-, and *C*-type bands, respectively.

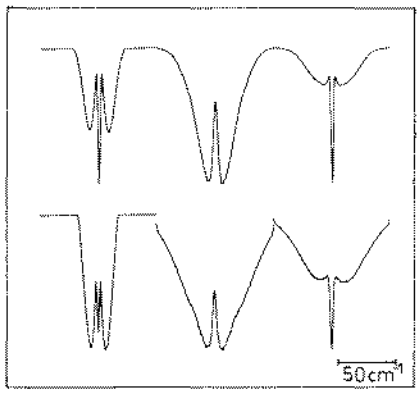

Fig. 8. Calculated i.r. vapour phase band contours for the *gauche* (top) and *anti* (bottom) conformations of azidoethane.

The assignment of the fundamental modes of vibration for the two conformations of azidoethane is admittedly closely connected with the development of the scaled quantum mechanical force fields [17]. However, analogies with the vibrational spectra of the haloethanes [29–35], of the isoelectronic compound isocyanatoethane [36] and the related isothiocyanatoethane [37, 38] as well as with thiocyanatoethane [39, 40] have been important in the starting phase and a close parallelism is found for the frequencies of vibration localized in the ethyl group.

We have previously mentioned that a few bands present in the spectra of the matrix isolated molecule, the vapour and the liquid vanish in the spectra of the crystalline solid and that these bands in the nitrogen matrix spectra all decrease in intensity upon annealing (Table 1). Hence, it is easy to divide most of the bands below 1400 cm^{-1} into two groups. Above 1400 cm^{-1} the fundamentals of the two conformers are expected to overlap and the same unambiguous distinction is not possible.

In order to determine which conformer remains in the crystal we have traditionally used the i.r. vapour phase contours (Fig. 8) and the Raman polarization data. Unfortunately, both types of spectral information are of limited help in the present case, the former because of overlapping bands and the latter because all the crucial bands, with only two exceptions, are expected to be polarized no matter the conformational interpretation. One of the exceptions is an ethyl rocking mode of a'' symmetry in the *anti* conformer and its corresponding mode in the *gauche* conformer, both expected around 800 cm^{-1}. There are two candidates in the matrix spectra, 805 and 799 cm^{-1} (N_2 matrix), two in the i.r. spectrum of the liquid, 815 and 796 cm^{-1}, but only one band in the Raman spectrum of the liquid, 798 cm^{-1}, which is weak, but definitely polarized. The Raman band corresponding to the i.r. band at 815 cm^{-1} (liq.) is probably hidden under the wing of the much more intense band at 847 cm^{-1} (see Fig. 6). With this explanation, the 805 cm^{-1} band must correspond to the a'' mode of the *anti* conformer and

Table 1. Vibrational spectral data* for azidoethane

Infra-red					Raman		Interpretation	
Argon matrix (12 K)	Nitrogen matrix (12 K)	Vapour (315 K)		Liquid (300 K)	Cryst. solid (80 K)	Liquid (220 K)	Cryst. solid (90 K)	*anti*	*gauche*
		~3005							
3001 m	~3000 w, sh ↑	3000 *Q*	m		2996 s		2997 s		ν_1
2994 s	2995 s ↓	2994 *Q*						ν_{16} (a'')	
2988 s	2988 m	2988 *Q*		2982 s	2980 s	2984 m	2982 vs	ν_1 (a')	ν_2
2978 w	2976 w ↑	~2980			2971 m		2973 vs		ν_3
2950 vw	2952 m	2956			2945 s		2946 s	ν_{17} (a'')	ν_4
				2938 s		2940 vs, *P*			
2945 m	2943 m	~2940			2936 w		2938 s		ν_5
2928 vw	2929 w ↓	~2920 *Q*		~2915 m	2918 vw	2918 s, *P*	2915 m	ν_2 (a')	comb.
2905 vw	2910 w ↓	2900					2904 sh	ν_3 (a')	comb.
2895 m	2898 w ↑								comb.
	2887 s ↓	2891 *Q*	s	~2886 s, sh	2890 m, br	2888 m, sh	2893 w	comb.	comb.
2882 m	2880 w ↑	2880		2876 s	2870 m	2875 s, *P*	2871 m	comb.	comb.
2192 s				2187 s	2187 s				
		~2155							
2146 s	2145 vs	2145		~2140 vs, sh	2144 vs				
2125 vs	2127 vs	2126			2130 vs				
2113 vvs	2114 vs	2118 *Q*	vs	2110 vvs	2122 vs	2110 w, *P*	2106 w	ν_4 (a')	ν_6
		2110			2109 vs				
		2097							
2088 s	2085 vs	2083		~2085 vs, sh	2089 vs		2090 w		
2071 vs	2074 s ↑	2068		2070 vs	2071 vs	2070 w	2069 m		
2050 w									
2037 w									
1475 m		1476							
1471 m	1471 ms	1466 *Q*	m	1465 s	1467 s	1469 w, sh	1471 m	ν_5 (a')	ν_7
1465 m	1464 vw ↑				1464 s		1464 w		ν_8
1460 w	1460 w ↓	1458 *Q*	m					ν_6 (a')	
1453 m	1450 ms	1454 *Q*	m	1449 s	1450 m	1452 m	1449 s	ν_{18} (a'')	ν_9
1450 m		1450			1442 m		1442 w	comb.	comb.
	1411 vw	~1405 w		~1400 m, sh	1394 w				

Table 1. (*Continued*)

Infra-red				Raman		Interpretation	
Argon matrix (12 K)	Nitrogen matrix (12 K)	Vapour (315 K)	Liquid (300 K)	Cryst. solid (80 K)	Liquid (220 K)	Cryst. solid (90 K)	*anti*	*gauche*
		1394						
1388 m	1388 s ↓	1388 *Q*	m, *AB*	1381 s	1378 m	1385 vw	1377 vw	ν_7 (a')	ν_{10}
1382 s	1382 w ↑	1383 *Q*							
		~1380							
1352 w	1355 vw								
		1352							
1347 s	1345 s ↓	1346 *Q*	s, *AB*	1342 s	1344 m	1348 m, *P*	1344 w	ν_8 (a')	ν_{11}
1341 w	1337 vw ↑								
		1338							
1314 m, br	1310 w ↑	~1310 w, *B*?			1305 m		~1306 vw		comb.
1293 s	1291 m								
		1294							
1285 s	1286 vs ↑	1288 *Q*	vs, *AB*	1283 vs	1288 vs	1284 m, *P*	1286 w	ν_9 (a')	ν_{12}
1281 s	1283 vs	1285 *Q*							
1279 vs	1279 vs ↓	1276							
1266 m									
1256 s			~1250 vs, sh		1252 m		1254 w		comb.
		1249							
1246 vs	1249 s ↑	1241 *Q*	vs, *AB*	1240 vs	1243 s	1242 m, *P*	1244 ms	ν_{19} (a'')	ν_{13}
1240 s	1240 vs ↓	1235							
		1144							
1132 s	1139 w ↑	1139 *Q*	m, *A*	1131 s	1138 m	1135 w	1137 w		ν_{14}
		1128			~1125 w, sh				comb.
1120 w	1124 mw ↓	1121 *Q*	m, *AB*	~1115 m, sh	*			ν_{10} (a')	
		1111							
1104 mw	1107 m ↓	1103 *Q*	w	1097 m	1090 w	1097 w, sh	1088 vw	ν_{20} (a'')	comb.
		~1095							
1080 s	1081 w ↑	1081 *Q*	m, *C*	1080 s	1075 m	1080 m, *P*	1074 m		ν_{15}
		1073							
1024 mw	1022 ms ↓	~1020 w, *B*?		1008 m	*	1010 w, sh	*	ν_{11} (a')	
		999							
987 s	990 mw ↑	993 *Q*	m, *AB*	989 s	988 m	989 m	989 vs		ν_{16}
		988							

				~900 vw					
		854							
846 mw	857 m ↓								
841 m	845 w ↑	848 *Q*	w, *AB*	843 m	844 s	843 s, *P*	847 s	ν_{12} (a')	ν_{17}
		842							
		806							
806 vw	805 w ↓			815 w, sh	*			ν_{21} (a'')	
794 s	799 w	797 *Q*	w	796 m	792 s	798 m, *P*	796 m		ν_{18}
		792							
		762 w		761 w				$CHCl_3$	
		666							
661 m	657 w, br ↑		m, *B*	659 s	648 m	659 m, *P*	651 m		ν_{19}
		650							
632 w	630 m ↓	630	w, *B*	637 m	*	635 m, *P*	*	ν_{13} (a')	
		568							
564 m	565 mw ↑	563 *Q*							
560 m	562 mw ↓	560 *Q*	w	557 m	562 m	561 vw	564 vw	ν_{21} (a'')	ν_{20}
		550							
		404							
410 mw	406 vw ↑		w, *B*	408 m	406 s	406 w, sh	406 mw		ν_{21}
		392							
	390 w ↓	385	*Q*, w, *A*	390 m	*	389 m, *P*	*	ν_{14} (a')	
		380							
	303 w ↑	~260 w		263 m, br	290 m	264 m	292 m		ν_{22}
	217 ms	~190 w		203 m	211 m	201 s	217 s	ν_{15} (a')	ν_{23}
					102 m		102 s		
							81 vs		
							68 vs		
				~55 m, br			46 m	ν_{24} (a'')?	ν_{24}?
							30 m		

* Weak bands in the regions 4000–3100, 2800–2200 and 2000–1700 cm^{-1} have been omitted.

† Abbreviations: s, strong; m, medium; w, weak; v, very; br, broad; sh, shoulder; *A*, *B*, and *C* denote band contours.

SA 44/4A-F

the 799 cm^{-1} band to the corresponding mode of the *gauche* conformer. And, since the 805 cm^{-1} band is missing in the spectra of the crystalline solid, it is the *gauche* conformer that remains in the crystal.

The other exception is found among the band pairs at 1139/1124 and 1107/1081 cm^{-1} (N_2 matrix). However, in this case, one of the components (1107) seems not to vanish completely in the spectra of the crystalline solid but apparently only decreases in intensity by an order of magnitude and at the same time shifts considerably towards lower wavenumbers. The weak band in the spectra of the crystalline solid can be explained by a binary combination and the correspondence between bands in the nitrogen matrix that decrease in intensity upon annealing and bands that vanish in the spectra of the crystalline solid is maintained. Now, two bands for each conformer are expected around 1100 cm^{-1}, all corresponding to rocking modes of the ethyl group. In the *gauche* conformation these two modes obviously have to be of the same symmetry, but for the *anti* form the two vibrations belong to different symmetry species. The i.r. vapour phase contours and the Raman polarization data should allow an unambiguous assignment of the *a''* mode of the *anti* conformer. The two bands centered around 1139 and 1121 cm^{-1} both have *A/B* hybrid band contours and can be discarded as possible candidates, and the typical *C*-type band at 1081 cm^{-1} definitely has a polarized Raman counterpart. Hence, we are left with the weak *Q*-branch at 1103 cm^{-1}, with a corresponding Raman line as a weak shoulder, for which we have no polarization data, of the much more intense band at 1080 cm^{-1} as the only reasonable candidate for the *a''* mode of the *anti* conformer. This assignment is also consistent with the *gauche* conformer remaining in the crystal.

The azide group frequencies are found very near to what has been observed in azidomethane [41–43]. The N≡N (or antisymmetric NNN) stretching vibration at 2114 cm^{-1} (N_2 matrix), flanked by numerous combination bands enhanced by Fermi resonance, is the strongest band in the entire i.r. spectrum, followed by the very intense N=N (or symmetric NNN) stretching mode at 1286 and 1279 cm^{-1} for the *gauche* and *anti* conformers, respectively. The extreme intensities of these bands are also in agreement with the predictions of theoretical calculations [17]. However, the Raman intensities fall short in comparison as the two stretching modes appear with medium to weak intensity in this effect.

Of the remaining two azide vibrations, the NNN bending mode shows a pronounced conformational dependence, 657 cm^{-1} for the *gauche* and 630 cm^{-1} for the *anti* form, which should be compared with 666 cm^{-1} in azidomethane [41–43]. Finally, the N=N torsional mode (or the NNN out-of-plane bending), found at 560 cm^{-1} in azidomethane, shows nearly no conformational dependence, 565 and 562 cm^{-1} for the *gauche* and *anti* forms, respectively. In analogy with what has been observed for azidomethane [43, 44] the N=N torsional mode is very weak in the Raman effect. It may be noted in the present context (and added as a verification of our assignment) that the conformational dependence of the NNN bending mode is so specific that just about any force field calculation (see later) will predict the *gauche* fundamental to fall at higher wavenumbers than the corresponding *anti* mode.

Further comments on the vibrational assignment would be superfluous and only a reiteration of Tables 1, 8 and 9 in prose.

Conformational equilibria

In order to find the enthalpy difference between the two conformations we have studied the Raman spectrum of azidoethane as a liquid in the temperature range 140–290 K. A part of the spectra is reproduced in Fig. 6 revealing three band pairs that show a marked intensity change with temperature. Apparently the bands at 1010, 635 and 390 cm^{-1} assigned to the *anti* conformer gain in intensity relative to their *gauche* counterparts upon cooling. However, this is not true and the peak heights give misleading values for the intensity measurements as the linewidths for the *anti* and *gauche* conformers have rather different temperature coefficients. As an example, the half-width at half-height for the band at 635 cm^{-1} is *ca* 11.5 cm^{-1} at 290 K but only 5.5 cm^{-1} at 140 K while the corresponding numbers for the band at 660 cm^{-1} are *ca* 8.5 and 7.5 cm^{-1}. The integrated scattered intensities of the Raman bands in the 1050–300 cm^{-1} region have been evaluated using Lorentzian profile functions [45]. The relative intensities obtained in this way for the band pairs 1010 (*anti*)/995 (*gauche*), 635 (*anti*)/660 (*gauche*) and 390 (*anti*)/405 (*gauche*) cm^{-1} are listed in Table 2, from which the enthalpy difference, $\Delta H^0_{a\to g}$ (liq.), may be calculated to be $-1.15(5)$ kJ mol^{-1}; i.e. the *gauche* conformation is the more stable in the liquid.

Table 2. Raman integrated intensity data and conformational enthalpy difference for azidoethane in the liquid phase

Temperature (K)	$\frac{I^{anti}_{1010}}{I^{gauche}_{995}}$	$\frac{I^{anti}_{635}}{I^{gauche}_{660}}$	$\frac{I^{anti}_{390}}{I^{gauche}_{405}}$
290		1.21	
288		1.21	
277		1.18	
273		1.17	
271		1.19	
243		1.14	
241		1.09	
215		1.04	2.22
208	0.25	1.00	2.19
179	0.22	0.90	2.02
178	0.22	0.88	1.95
165	0.21	0.78	1.85
164	0.20	0.80	1.96
163	0.20	0.78	1.93
141	0.19	0.73	1.87
141	0.19	0.74	1.83
141	0.19	0.73	1.86

$\Delta H^0_{a\to g}$ (liq.) $= -1.15$ (5) kJ mol^{-1}.

It is highly informative that no bands vanish completely in the matrix spectra upon annealing, not even after more than 20 h at the highest possible annealing temperature for the matrix materials. Assuming that (1) the conformational equilibrium at room temperature is trapped in the nitrogen matrix and (2) the matrix materials do not change the conformational enthalpy difference, then it is possible to get an estimate of this value from the intensity ratio of individual band pairs before and after annealing. The first assumption is commonly accepted as valid if the barrier to rotational isomerism is not too low; the second assumption, however, cannot possibly be expected to be valid in general. The only experimental result that is in favour of this approximation in the present case is the fact that the relative intensities of the *gauche/anti* band pairs are approximately the same in the spectra of the annealed argon and nitrogen matrices. (An additional matrix isolation experiment using a hot nozzle or a Knudsen-cell would be an ideal solution to our dilemma, but, unfortunately, one would need such high nozzle temperatures that pyrolysis probably would be a severe obstacle.) In any case, the relative intensities of a few band pairs before and after annealing are listed in Table 3, from which the conformational enthalpy difference, $\Delta H^0_{a\to g}$ (N_2 matrix) $\approx \Delta H^0_{a\to g}$ (vap.), can be estimated as $-0.56(10)$ kJ mol^{-1}; i.e. the *gauche* conformation is the more stable form.

In conclusion, the conformation present in the crystal (*gauche*) is also the more stable in both the argon and nitrogen matrices and most probably also the more stable in the vapour phase as well. In the liquid phase the *gauche* conformation is the more stable form, the enthalpy difference being about twice as large as in the nitrogen matrix. However, in all phases the conformational enthalpy difference is small, as was also indicated by the *ab initio* calculations [17].

Barrier to rotational isomerism

As already mentioned, the spectra of azidoethane trapped in nitrogen and argon matrices are quite different with respect to the relative band intensities before annealing. Whereas the spectra of the argon matrix hardly change upon annealing, the spectra of the nitrogen matrix change significantly in such a manner that after annealing the spectra are nearly identical with those of the argon matrix. The conclusion to be drawn is that the barrier to rotational isomerism is so low in the argon matrix that the conformational equilibrium is established during the deposition. With a deposition temperature of 18 K this sets an upper limit to the barrier in the argon matrix of 6 kJ mol^{-1} [46].

Table 3. Relative band intensities before and after annealing of azidoethane in a nitrogen matrix

Band pair *anti/gauche*	Intensity ratio* R_B	Intensity ratio* R_A	R_A/R_B
1388/1382	6.4	0.77	0.12
1124/1139	1.9	0.30	0.15
1107/1076	7.0	1.00	0.14
1022/990	2.2	0.33	0.15
857/845	4.2	0.43	0.10
805/799	2.5	0.31	0.12
630/660	4.2	0.78	0.19
560/565	2.3	0.59	0.25
Mean value			0.15(5)

* Intensity data measured by peak height.

Subscripts A and B denote after and before annealing, respectively.

In Fig. 7 is shown a part of the nitrogen matrix spectrum before annealing, after 60 min and after 100 min of annealing at 32–35 K. The relative band intensities change visibly in the first 60–100 min of annealing, but then equilibrium seems to have been established. As the energy difference between the two conformations is small, the barrier height cannot be calculated in the usual way by assuming a simple first-order reaction with no reverse reaction, $A \to B$, and then applying the Arrhenius equation for calculating the activation energy/barrier height. It is necessary to take into account the reverse reaction, that is, the kinetics must satisfy the differential equations:

$$Dn_A = -k_A n_A + k_B n_B \quad \text{and} \quad Dn_B = k_A n_A - k_B n_B \qquad (1)$$

where: $D = \mathrm{d}/\mathrm{d}t$ and $n_A + n_B$ is constant.

With the introduction of mole fractions, $x_A = n_A/(n_A + n_B)$, in Eqn. (1):

$$Dx_A = -(k_A + k_B)x_A + k_B \quad \text{and}$$
$$Dx_B = -(k_A + k_B)x_B + k_A \qquad (2)$$

are obtained, which both have solutions of the type

$$\{x(t) - x^\infty\}/\{x^0 - x^\infty\} = \exp[-(k_A + k_B)t]. \qquad (3)$$

The time dependence of the individual band intensities is obviously then

$$\{I(t) - I^\infty\}/\{I^0 - I^\infty\} = \exp[-(k_A + k_B)t]. \qquad (4)$$

The constant $k_A + k_B$ may readily be obtained from an analysis of the spectral data shown in Table 4 and is found to be $4.9(10) \times 10^{-4}$ s^{-1}. Applying the Arrhenius equation, $k = A\exp(-E/RT)$, to the rate constants then gives

$$k_A + k_B = A\exp[-E/RT] + 2A\exp[-(E+\Delta)/RT] \qquad (5)$$
$$= \{1 + 2\exp(-\Delta/RT)\}\, A\exp(-E/RT),$$

where E is the barrier height from the *anti* to the *gauche* conformation and Δ the energy difference $E_{\text{anti}} - E_{\text{gauche}}$. Using $\Delta \approx 500$ J mol^{-1}, as was found in the previous paragraph, the extra factor in the modified Arrhenius equation becomes 1.3 at 32 K. Taking $A = 10^{11.2}$ s^{-1} [47] results in a barrier height $E = 9.0(10)$ kJ mol^{-1}, which is almost three times as large as was found by the theoretical calculations [17]. On the other hand, the barrier height is less than 6 kJ mol^{-1} in the argon matrix which may (or may not)

Table 4. Infra-red intensity data as a function of annealing time for selected bands of azidoethane isolated in a nitrogen matrix. Annealing temperature 32(2) K

Wavenumber	I_0	I_{60}	I_{100}	$\{I_{60}-I_{100}\}$ / $\{I_0-I_{100}\}$
1388	159	88	70	0.20
1382	25	76	91	0.09
1310	29	79	90	0.18
1139	24	59	64	0.13
1124	46	23	19	0.15
1107	70	38	28	0.24
1076	10	23	28	0.28
1022	99	45	32	0.11
990	45	91	96	0.10
857	80	27	17	0.16
845	19	38	40	0.09
805	53	23	18	0.14
799	21	53	59	0.16
657	16	28	32	0.25
630	67	32	25	0.22
565	34	69	75	0.17
562	79	51	44	0.20
Mean value				0.17(6)

Rate constant according to: $\{I(t)-I^\infty\}/\{I^0-I^\infty\} = \exp[-kt]$,
$k = 4.9(10)\times 10^{-4}\ s^{-1}$.

* Intensities measured by peak height in arbitrary units. Subscript denotes annealing time in min.

Table 5. Definition of internal symmetry co-ordinates for azidoethane with reference to Fig. 1

$S_1 = \Delta R_{12}$
$S_2 = \Delta R_{23}$
$S_3 = \Delta R_{34}$
$S_4 = \Delta R_{45}$
$S_5 = \{\Delta R_{46} + \Delta R_{47}\}^{1/2}$
$S_6 = \Delta R_{58}$
$S_7 = \{\Delta R_{59} + \Delta R_{50}\}^{1/2}$
$S_8 = \Delta\alpha_{123}$
$S_9 = \Delta\alpha_{234}$
$S_{10} = \Delta\alpha_{345}$
$S_{11} = \{\Delta\alpha_{346} + \Delta\alpha_{347}\}^{1/2}$
$S_{12} = \{\Delta\alpha_{546} + \Delta\alpha_{547}\}^{1/2}$
$S_{13} = \Delta\alpha_{458}$
$S_{14} = \{\Delta\alpha_{459} + \Delta\alpha_{450}\}^{1/2}$
$S_{15} = \{\Delta\alpha_{859} + \Delta\alpha_{850}\}^{1/2}$
$S_{16} = \{\Delta R_{46} - \Delta R_{47}\}^{1/2}$
$S_{17} = \{\Delta R_{59} - \Delta R_{50}\}^{1/2}$
$S_{18} = \{\Delta\alpha_{346} - \Delta\alpha_{347}\}^{1/2}$
$S_{19} = \{\Delta\alpha_{546} - \Delta\alpha_{547}\}^{1/2}$
$S_{20} = \{\Delta\alpha_{459} - \Delta\alpha_{450}\}^{1/2}$
$S_{21} = \{\Delta\alpha_{859} - \Delta\alpha_{850}\}^{1/2}$
$S_{22} = \Delta\tau_{1234}$
$S_{23} = \Delta\tau_{2345}$
$S_{24} = \{\Delta\tau_{3458} + \Delta\tau_{6450} + \Delta\tau_{7459}\}^{1/3}$

resemble the vapour phase more when it comes to barriers between rotational isomers.

Force constant calculations

The normal modes of vibration for the two conformations of azidoethane were calculated from scaled quantum mechanical (SQM) force fields [17]. The Cartesian co-ordinates were calculated from the structural parameters given in Fig. 3 in Ref. [17]. Definition of the internal symmetry co-ordinates is given in Table 5 with reference to the atomic numbering shown in Fig. 1. The internal symmetry co-ordinates, listed in Table 5, were chosen purely for practical reasons for the *ab initio* calculations and the least squares procedure outlined in Ref. [17]. Transformation of the force constants corresponding to any non-redundant set of symmetry co-ordinates obviously can easily be achieved by a linear transformation [48]. The SQM force fields are given in Tables 6 and 7 for the *anti* and *gauche* conformations, respectively. Finally, the observed and calculated fundamental modes of vibration are compared in Table 8 for the *anti* conformer and in Table 9 for the *gauche* conformer.

Prior to the *ab initio* calculation of the force fields and the empirical scaling of these [17] we performed a number of normal co-ordinate calculations based upon a common force field constructed by transferring force constants from the standard *n*-alkyl chloride valence force field of SNYDER and SCHACHTSCHNEIDER [49] and a proposed force field of azidomethane [50]. Although it often is possible to adjust a reasonable force field in such a way that it apparently supports a proposed vibrational assignment for two conformations of a molecule, it is, unfortunately, also possible, often with only minor modifications to the same force field, to support the reverse conformational interpretation. With one exception, this was also true in the present case, but regardless of any reasonable modification to the transferred valence force field the NNN bending mode of the *gauche* conformer was always calculated at higher wavenumbers than the corresponding mode in the *anti* form. This is, in our opinion, a valuable piece of circumstantial evidence in favour of our conformation assignment.

In contrast to the equivocal standard force constant calculations, the conformational specificity of the SQM force fields and the correspondingly calculated normal modes of vibration is much more pronounced and not just limited to the NNN bending modes. As a matter of fact, a reversal of our conformational assignment is quite unacceptable within the approximation of the model. However, in accepting the (sad) fact that there is nothing divine about force fields calculated by quantum mechanical methods on the SCF level, and in making allowance for the profane least squares procedure employed in scaling the force fields [17] we risk branding ourselves as simpletons advocating this approach to conformational analysis. However, in our opinion, the results from applying the SQM azide force fields [15, 16, 18–21] have so far been promising.

Table 6. Scaled quantum mechanical force field* for the *anti* conformation of azidoethane

17.073														
1.805	9.667			Species a'										
−0.150	0.178	4.231												
−0.043	0.037	0.188	4.482											
0.065	−0.018	0.214	0.104	4.768										
0.009	0.012	0.002	0.061	0.016	4.839									
−0.002	−0.015	0.009	0.088	−0.002	0.058	4.930								
−0.070	0.228	−0.017	0.012	−0.013	−0.002	0.005	0.629							
−0.107	0.725	0.516	0.056	−0.003	0.006	0.009	0.100	0.874						
−0.031	0.289	0.541	0.373	−0.233	0.067	−0.055	0.008	0.144	1.902					
0.121	−0.181	0.598	0.003	−0.224	0.004	−0.003	0.009	−0.016	0.812	1.731				
−0.034	0.046	−0.049	0.399	−0.205	0.002	0.025	−0.011	−0.010	0.827	0.961	1.606			
0.012	0.037	0.082	0.259	0.000	0.152	−0.212	0.007	0.035	0.143	−0.007	−0.038	1.221		
−0.015	−0.014	−0.044	0.438	0.020	0.009	−0.178	0.001	−0.006	−0.089	−0.006	0.072	0.816	1.765	
0.010	0.003	0.006	0.002	−0.003	0.217	−0.162	−0.003	−0.009	0.009	−0.005	0.003	0.815	1.132	1.627
4.646														
0.023	4.848			Species a''										
0.064	−0.019	0.719												
0.118	−0.042	0.017	0.625											
−0.039	0.126	−0.001	−0.134	0.662										
−0.001	0.148	0.005	0.001	0.028	0.532									
0.002	0.001	−0.003	0.002	0.000	0.000	0.008								
−0.009	0.003	−0.028	0.002	0.002	−0.002	0.002	0.016							
0.002	−0.008	−0.008	−0.003	−0.030	−0.011	0.000	−0.005	0.029						

* Units: stretch and stretch–stretch constants in mdyn Å^{-1}; stretch–bend constants in mdyn Å rad^{-1}; bend and bend–bend constants in mdyn Å rad^{-2}.

Table 7. Scaled quantum mechanical force field* for the *gauche* conformation of azidoethane

17.115																							
1.799	9.484																						
−0.152	0.228	4.275																					
0.031	−0.018	0.258	4.172																				
0.029	−0.020	0.143	0.109	4.912																			
0.017	−0.026	−0.001	0.060	0.017	4.805																		
0.014	0.003	0.029	0.094	−0.003	0.060	4.875																	
−0.071	0.248	−0.024	0.000	−0.002	0.002	0.001	0.629																
−0.098	0.740	0.562	−0.001	0.022	−0.007	0.009	0.102	0.911															
0.120	−0.172	0.526	0.291	−0.223	0.062	−0.038	0.019	0.021	1.967														
0.078	−0.009	0.649	0.017	−0.197	0.004	0.002	0.024	0.075	1.028	1.940													
0.016	−0.030	0.011	0.419	−0.182	0.002	0.026	0.007	0.003	1.035	1.229	1.853												
0.037	−0.050	0.085	0.236	0.003	0.142	−0.216	0.007	0.001	0.137	−0.008	−0.041	1.209											
0.003	0.015	−0.033	0.416	0.020	0.008	−0.186	−0.001	0.009	−0.092	−0.007	0.072	0.818	1.754										
0.001	−0.012	0.006	0.013	−0.006	0.217	−0.157	0.003	−0.004	−0.016	−0.003	0.006	0.823	1.121	1.626									
−0.041	−0.012	−0.050	−0.003	0.149	−0.001	−0.002	0.015	0.034	0.009	0.022	−0.002	−0.003	−0.002	−0.004	4.818								
−0.019	−0.003	−0.009	−0.007	0.000	−0.004	0.047	0.001	−0.005	−0.013	0.002	0.001	0.005	0.006	0.000	0.021	4.791							
−0.072	0.257	0.016	−0.004	0.019	−0.001	0.005	0.006	0.102	−0.076	−0.065	−0.082	−0.003	−0.001	−0.001	0.084	−0.018	0.801						
−0.012	0.040	−0.029	0.006	−0.003	−0.002	0.001	−0.015	−0.005	−0.062	−0.090	−0.064	−0.003	0.002	0.001	0.119	−0.041	0.084	0.647					
−0.023	−0.007	−0.008	0.006	0.002	−0.001	−0.001	0.005	−0.009	−0.009	0.001	0.003	0.002	−0.002	0.007	−0.037	0.120	−0.004	−0.133	0.644				
0.013	−0.006	0.005	0.008	−0.001	−0.002	−0.008	0.001	0.003	0.010	−0.001	0.000	−0.003	0.007	−0.004	0.000	0.152	0.002	0.001	0.019	0.540			
0.000	0.000	−0.002	0.000	0.001	0.000	0.000	−0.001	0.000	0.002	−0.003	−0.002	0.001	−0.001	0.000	−0.001	0.000	0.001	0.001	0.001	0.000	0.008		
−0.005	0.009	0.005	0.019	−0.008	−0.011	0.048	−0.002	0.003	0.074	−0.022	0.005	−0.039	−0.072	−0.002	−0.006	−0.028	0.005	0.011	0.010	0.017	0.002	0.028	
−0.003	0.010	0.001	−0.001	0.000	−0.001	0.002	−0.002	0.003	0.002	0.000	0.000	−0.003	−0.011	−0.005	0.001	−0.003	−0.006	−0.003	−0.021	−0.015	0.000	0.001	0.032

*Units: stretch and stretch–stretch constants in mdyn Å^{-1}; stretch–bend constants in mdyn Å rad^{-1}; bend and bend–bend constants in mdyn Å rad^{-2}.

Table 8. Observed and calculated fundamental frequencies (cm^{-1}) of the *anti* conformation of azidoethane

Observed*	Calculated	Description
a'		
2988	2988	CH_3 asym. stretch
2929	2926	CH_3 sym. stretch
2910	2901	CH_2 sym. stretch
2114	2106	N≡N stretch
1471	1490	CH_2 scissor
1460	1463	CH_3 asym. def.
1388	1389	CH_3 sym. def.
1345	1334	CH_2 wag
1279	1298	N=N stretch
1124	1116	CH_3 rock
1022	1023	C–C stretch
857	854	N–C stretch
630	633	N≡N=N i.p. bend
390	394	N–C–C bend
190†	190	N=N–C bend
a''		
2996	2999	CH_3 asym. stretch
2952	2938	CH_2 asym. stretch
1450	1444	CH_3 asym. def.
1240	1259	CH_2 twist
1107	1105	CH_3/CH_2 rock
805	803	CH_2/CH_3 rock
562	565	N=N torsion
—	225	CH_3 torsion
55‡	42	C–N torsion

*Frequencies from N_2 matrix i.r. spectra except when noted.
†From vapour phase.
‡From liquid phase.

Table 9. Observed and calculated fundamental frequencies (cm^{-1}) of the *gauche* conformation of azidoethane

Observed*	Calculated	Description
3000	3025	CH_2 asym. stretch
2988	2988	CH_3 asym. stretch
2976	2964	CH_3 asym. stretch
2952	2919	CH_2 sym. stretch
2943	2910	CH_3 sym. stretch
2114	2104	N≡N stretch
1471	1488	CH_2 scissor
1464	1460	CH_3 asym. def
1450	1459	CH_3 asym. def
1382	1384	CH_3 sym. def.
1337	1337	CH_2 wag
1286	1292	N=N stretch
1249	1253	CH_2 twist
1139	1124	CH_3/CH_2 rock
1081	1081	CH_3 rock
990	989	C–C stretch
845	847	C–N stretch
799	807	CH_2/CH_3 rock
657	656	N≡N=N i.p. bend
565	561	N=N torsion
406	405	C–N–N bend
260†	260	C–N=N bend/CH_3 torsion
190†	179	C–N=N bend/CH_3 torsion
55‡	58	C–N torsion

*Frequencies from N_2 matrix i.r. spectra except when noted.
†From vapour phase.
‡From liquid phase.

Acknowledgements—The authors wish to thank Perkin–Elmer (Norway) for the opportunity to test and use one of their instruments under laboratory conditions. We are also grateful to ANNE HORN for drawing the figures. H. P. received a postdoctoral fellowship from DEMINEX through NTNF and K. K. received a grant through the Cultural Exchange Program between Hungary and Norway.

REFERENCES

[1] H. STAUDINGER and E. HAUSER, *Helv. Chim. Acta* **4**, 861 (1921).
[2] M. E. BURNS and R. H. SMITH, JR, *Chem. Engng News* **63**(40), 2 (1985).
[3] H. O. SPAUSCHUS and J. M. SCOTT, *J. Am. chem. Soc.* **77**, 210 (1951).
[4] E. A. SHOTT-L'VOVA and YA. K. SYRKIN, *Dokl. Akad. Nauk SSSR* **87**, 639 (1952).
[5] YU. N. SHEINKER, *Dokl. Akad. Nauk SSSR* **77**, 1043 (1951).
[6] E. LIEBER, C. N. RAMACHANDRA RAO, T. S. CHAO and W. H. WAHL, *J. sci. ind. Res.* **16B**, 95 (1957).
[7] T. KANDA, Y. SAITO and K. KAWAMURA, *Bull. chem. Soc. Jpn.* **35**, 172 (1962).
[8] M. WITANOWSKI, *J. Am. chem. Soc.* **90**, 5683 (1968).
[9] M. WITANOWSKI, L. STEFANIAK and G. A. WEBB, *J. magn. Reson.* **36**, 227 (1979).
[10] V. V. MELNIKOV, S. A. ZACHESLAVSKII, L. F. BAEVA and B. V. GIDASPOV, *Zh. org. Khim.* **8**, 1805 (1972).
[11] YU. N. SHEINKER and YA. K. SYRKIN, *Izv. Akad. Nauk SSSR Ser. Fiz.* **14**, 478 (1950).
[12] V. V. MELNIKOV, L. F. BAEVA and B. V. GIDASPOV, *Zh. Prikl. Spektrosk.* **18**, 87 (1973).
[13] I. STOLKIN, T.-K. HA and HS. H. GÜNTHARD, *Chem. Phys.* **21**, 21 (1977).
[14] P. KLAEBOE, C. J. NIELSEN, H. PRIEBE, S. H. SCHEI and C. E. SJØGREN, *J. molec. Struct.* **141**, 161 (1986).
[15] S. H. SCHEI, H. PRIEBE, C. J. NIELSEN and P. KLAEBOE, *J. molec. Struct.* **147**, 203 (1986).
[16] C. J. NIELSEN, P. KLAEBOE, H. PRIEBE and S. H. SCHEI, *J. molec. Struct.* **147**, 217 (1986).
[17] C. J. NIELSEN and C. E. SJØGREN, *J. molec. Struct. Theochem.* **150**, 361 (1987).
[18] J. ALMLOF, G. O. BRAATHEN, P. KLAEBOE, C. J. NIELSEN, H. PRIEBE and S. H. SCHEI, *J. molec. Struct.* **160**, 1 (1987).
[19] P. KLAEBOE, K. KOSA, C. J. NIELSEN, H. PRIEBE and S. H. SCHEI, *J. molec. Struct.* (submitted).
[20] C. J. NIELSEN, H. PRIEBE, R. SALZER and S. H. SCHEI, *J. molec. Struct.* (in press).
[21] P. KLAEBOE, K. KOSA, C. J. NIELSEN, H. PRIEBE and S. H. SCHEI, *J. molec. Struct.* (to be published).
[22] B. P. WINNEWISSER, *J. molec. Spectrosc.* **82**, 220 (1980).
[23] K. O. CHRISTE, D. CHRISTEN, H. OBERHAMMER and C. S. SCHACK, *Inorg. Chem.* **23**, 4283 (1984).
[24] A. ALMENNINGEN, B. BAK, P. JANSEN and T. G. STRAND, *Acta chem. Scand.* **27**, 1531 (1973).
[25] C. J. NIELSEN, A. GATIAL and H. PRIEBE (to be published).
[26] D. J. DEFREES, G. H. LOEW and A. D. MCLEAN, *Astrophys. J.* **254**, 405 (1982).
[27] F. A. MILLER and B. M. HARNEY, *Appl. Spectrosc.* **24**, 291 (1970).
[28] T. UEDA and T. SHIMANOUCHI, *J. molec. Spectrosc.* **28**, 350 (1968).
[29] O. SAUR, J. TRAVERT, J. SAUSSEY and J.-C. LAVALLEY, *J. Chim. phys.* **72**, 907 (1975).
[30] F. A. MILLER and F. E. KIVIAT, *Spectrochim. Acta* **25A**, 1363 (1969).
[31] R. GAUFRÈS and M. BÉJAUD-BIANCHI, *Spectrochim. Acta* **27A**, 2249 (1971).
[32] G. A. CROWDER, *J. molec. Spectrosc.* **48**, 467 (1973).
[33] J. R. DURIG, J. W. THOMPSON, V. W. THYAGESAN and

J. D. WITT, *J. molec. Struct.* **24**, 41 (1975).
[34] F. WINTHER and D. O. HUMMEL, *Spectrochim. Acta* **25A**, 425 (1969).
[35] D. C. MCKEAN, J. C. LAVALLEY, O. SAUR and J. TRAVERT, *Spectrochim. Acta* **33A**, 865 (1977).
[36] R. P. HIRSCHMANN, R. N. KNISELEY and V. A. FASSEL, *Spectrochim. Acta* **21**, 2125 (1965).
[37] J. R. DURIG, H. L. HEUSEL, J. F. SULLIVAN and S. CRADOCK, *Spectrochim. Acta* **40A**, 739 (1984).
[38] J. R. DURIG, J. F. SULLIVAN, D. T. DURIG and S. CRADOCK, *Can. J. Chem.* **63**, 2000 (1985).
[39] J. R. DURIG, J. F. SULLIVAN and S. CRADOCK, *J. phys. Chem.* **88**, 374 (1984).
[40] G. O. BRAATHEN and A. GATIAL, *Spectrochim. Acta* **42A**, 615 (1986).
[41] E. MANTICA and G. ZERBI, *Gazz. Chim. Ital.* **90**, 53 (1960).
[42] F. A. MILLER and D. BASSI, *Spectrochim. Acta* **19**, 565 (1963).
[43] C. J. NIELSEN, F. M. NICOLAISEN and H. PRIEBE (unpublished results).
[44] L. KAHOVEC, K. W. KOHLRAUSCH, A. W. REITZ and J. WAGNER, *Z. phys. Chem. Leipzig* **B39**, 431 (1938).
[45] D. SÜLZLE, *The Program PROFILE*. Department of Chemistry, University of Oslo (1987).
[46] A. J. BARNES, *J. molec. Struct.* **113**, 161 (1984).
[47] R. PONG, T. D. GOLDFARB and A. KRANTZ, *Ber. bunsenges. phys. Chem.* **82**, 9 (1978).
[48] S. J. CYVIN (editor), in *Molecular Structure and Vibrations*, Ch. 6. Elsevier, Amsterdam (1972).
[49] R. G. SNYDER and J. H. SCHACHTSCHNEIDER, *J. molec. Spectrosc.* **30**, 290 (1969).
[50] W. T. THOMPSON and W. H. FLETCHER, *Spectrochim. Acta* **22**, 1907 (1966).